Interference and Outage in Random D2D Networks under Millimeter Wave Channels

S. Kusaladharma and C. Tellambura, *Fellow*, *IEEE*
Department of Electrical and Computer Engineering
University of Alberta, Edmonton, Alberta T6G 2V4, Canada
Email: kusaladh@ualberta.ca and chintha@ece.ualberta.ca

***Abstract*—Millimeter wave communication is a promising concept for the fifth generation (5G) of cellular wireless networks due to the large available bandwidth while device to device (D2D) communication among nearby devices which saves network resources is also gaining attention. As such, D2D networks underlaying millimeter wave cellular systems hold massive potential. However, the performance of such a D2D network incorporating spatial randomness and power control has not yet been characterized. To fill this knowledge gap, we develop a comprehensive analysis of the performance of a D2D receiver. To this end, we model cellular transmitters and receivers as homogeneous Poisson point processes and the D2D network as a Matern cluster process, and incorporate blockages due to random objects, sectored antenna patterns, log-distance path loss, and Nakagami-m fading. Furthermore, we consider path loss and antenna gain inversion based power control, and peak power constraints for D2D devices along with distinct path loss exponents and fading severities for line-of-sight and non-line-of-sight scenarios. With the aid of stochastic geometry tools, we derive closed-form expressions of the moment generating function of the aggregate interference experienced by a D2D receiver and its outage probability. We finally show that the feasibility of millimeter wave D2D communication relies heavily on the D2D cluster radii, peak power thresholds, and node densities.**

***Index Terms*—Millimeter wave networks, D2D networks, Stochastic geometry, aggregate interference**

I. Introduction

Due to the scarcity of unallocated spectrum within the conventional microwave bands, millimeter wave communication in the $30 - 300$ GHz band has emerged as one of the most promising technologies for the fifth generation (5G) of cellular communication [1], [2]. The high bandwidth and sparse existing usage make millimeter wave communication highly attractive. Furthermore, the reduced antenna sizes at these frequencies enable a large number of antenna elements within a small space, and thus provide exciting prospects for other candidate technologies such as massive multiple-input multiple-output (MIMO). This in turn will potentially reduce out of cell interference, and provide beamforming gains for the desired links. Moreover, standardization has already occurred under IEEE 802.15.3c and IEEE 802.11ad for the 60 GHz band [3]. However, high path loss, the sensitivity to blockages, atmospheric absorption, and high noise powers provide significant challenges to successfully incorporating millimeter wave frequencies.

On another note, device-to-device (D2D) networks underlaying the cellular network enable transmissions between neighbouring devices for certain applications which saves transmission power and network resources [4]. When certain services require local access for high rate services, direct communication between the users instead of using the cellular network is the most efficient solution [5]. Moreover, a D2D transmission can become a relay link for cell-edge users to connect with a base station. Thus, enabling D2D communications has also been a cornerstone for 5G research [6], and integrating millimeter wave with D2D networking is an exciting prospect [5]. However, underlaying D2D onto a cellular network provides challenges with respect to interference management, and the peculiarities of the millimeter wave channel exemplify the challenge regarding coverage.

A. Related Work

Research on millimeter wave cellular networks has received significant attention in the recent years. Reference [7] considers the possibility of base station downlink co-operation to reduce the outage probability, and concludes that co-operation significantly improves the performance in dense networks without small scale fading. However, the authors show that the performance improvement is minimal in less dense networks with Rayleigh fading. A general framework to evaluate the coverage and rate in millimeter wave networks is proposed in [3], [8], and the case of dense networks is investigated further in [3] where the line of sight region is approximated with a ball. It is concluded that dense networks achieve similar coverage and significantly higher data rates with respect to conventional cellular networks. In contrast, [8] proposes a mathematical framework which accounts for the interference from other cells in ultra-dense deployments.

The research on millimeter wave networks has also incorporated D2D networks. Reference [9] considers stochastic geometry to analyze wearable D2D networks within a finite region, and concludes that millimeter wave frequencies provide significant throughput gain even with omni-directional antennas. Furthermore [10] proposes an efficient scheduling scheme for millimeter wave small cells while exploiting D2D links for efficiency while [11] studies the spatial heterogeneity of outdoor users via the coefficient of variation. Moreover, [12] proposes a resource allocation scheme for underlaid D2D networks within the E-band, and shows that the proposed solution increases throughput while reducing interference.

B. Motivation and Contribution

In this work, we aim to characterize the outage performance of a D2D network underlaid upon a millimeter wave cellular network. While millimeter wave frequencies will present lower interference due to directionality, there would be degradation

to the desired signal due to blockages. Moreover, how log-distance path loss and peak power constraints affect the performance under millimeter wave frequencies are open issues. In addition, ubiquitous networks are increasingly irregular. As such, stochastic models incorporating spatial randomness need to be taken into account.

In this work, we model the cellular base stations and users as independent homogeneous Poisson point processes and the D2D network as a Matern cluster process in $\mathbb{R}^2$ to incorporate spatial randomness. A simplified Boolean blockage model is assumed, and line-of-sight (LOS) and non-line-of-sight (NLOS) conditions are modelled separately with different log-distance path loss exponents and Nakagami fading parameters. Moreover, directional antenna patterns are assumed for all devices, and antenna alignment takes place before any data transmission attempt. Each cellular user is assumed to connect to its nearest base station while a D2D receiver connects with the transmitter corresponding to the cluster head. We assume a path loss and antenna gain inversion based power control model where the D2D network is also peak power constrained.

Our main contributions of this paper are listed below:

- The moment generating function (MGF) of the interference to a D2D receiver from other D2D transmitters and cellular base stations is derived using stochastic geometry based tools. More precisely, the Mapping and Marking theorems relating to Poisson point processes are used to transform the process of interfering base stations into an equivalent inhomogeneous process which incorporates blockage, antenna gains, transmit power, fading, and path loss variations.
- The outage performance of a D2D receiver is derived in closed-form while taking into account the constraints due to peak power constraints and random blockages.

Notations: $\Gamma(x,a) = \int_a^\infty t^{x-1}e^{-t}dt$ and $\Gamma(x) = \Gamma(x,0)$ [13]. $\Pr[A]$ is the probability of event A, $f_X(\cdot)$ is the probability density function (PDF), $F_X(\cdot)$ is the cumulative distribution function (CDF), $M_X(\cdot)$ is the MGF, $M_X^(k)(\cdot)$ is the k-th derivative of the MGF, and $\mathbb{E}_X[\cdot]$ denotes the expectation over random variable X.

II. System Model and Assumptions

This section introduces the system parameters and models used throughout the rest of the paper.

A. Spatial Distribution and Blockages

We consider four separate types of nodes: 1) cellular base stations, 2) cellular users, 3) D2D transmitters, and 4) D2D receivers. While the D2D transmitters/receivers in principle can also be cellular users, we differentiate them in this research for the ease of analysis. The cellular base stations and users are modelled as two independent, stationary homogeneous Poisson point processes in $\mathbb{R}^2$. The homogeneous Poisson point process has been used widely in literature to model wireless nodes, and has been shown to be an extremely accurate model [14], [15]. With a homogeneous Poisson point process, the number of nodes within any given area $\mathcal{A}$ is given by [16]

$$\Pr[N(\mathcal{A}) = n] = \frac{(\lambda\mathcal{A})^n}{n!}e^{-\lambda\mathcal{A}}, \tag{1}$$

where λ is the average node density per unit area. Due to the homogeneity, λ is constant and location independent. As such, the processes of cellular base stations and users are respectively denoted as $\Phi_{c,b}$ and $\Phi_{c,u}$ having densities of $\lambda_{c,b}$ and $\lambda_{c,u}$ respectively.

The D2D network is modelled as a Matern cluster process [17]. Within a Matern cluster process, multiple clusters exist in $\mathbb{R}^2$ where the cluster centers are distributed as a homogeneous Poisson point process and each cluster center is encircled by a daughter process existing within a ball of radius R from it[1]. The daughter processes are homogeneous within their respective annular regions and independent of each other. In our case the cluster centers having a density of $\lambda_{d,t}$ model the D2D transmitters and the daughter nodes having a density of $\lambda_{d,r}$ model the D2D receivers[2].

An important factor to consider in millimeter wave networks is the signal blockage from random objects which significantly impacts the received signal characteristics. We will model the blockages stochastically using a rectangular Boolean scheme [18], and the blockages are assumed to be stationary and isotropic. With these assumptions, the probability of a link of length r with no blockage (LOS link) is given by $e^{-\beta r}$, where β is a constant relating to the size and density of the blockages. Similarly, the probability of a NLOS link is given by $1-e^{-\beta r}$. It is readily observed that a link is more susceptible to blockage as its length increases. Moreover, for mathematical tractability, we assume that the effect of blockage on different links is independent. Note that the different types of nodes have a chance of falling within the environs of a blocking object. However, although we omit such a scenario, it can be readily incorporated to our analysis through independently thinning the different processes of nodes [3].

B. Channel Model and Antenna Pattern

The cellular system is assumed to employ universal frequency reuse, and the same set of cellular frequencies are also used by D2D users. For mathematical tractability, we assume that the channel gains are independent of the underlying spatial process of nodes. We consider path loss and small scale fading for all the links. However, the parameters of these vary depending on the LOS or NLOS nature of the link.

From the model [19], we write the general path loss for a millimeter wave link of distance r as $PL(r) = c_s r^{\alpha_s}$, where $s \in \{L, N\}$, and L, N correspond to LOS and NLOS links. The parameter α_s is the path loss exponent while c_s is the

[1]Note that this system model is analogous to a homogeneous Poisson point process of D2D receivers where the transmitters only select a receiver within a given radius.

[2]We assume that each daughter process has the same constant density.

intercept. The small fading is assumed to be Nakagami. Thus, the channel power gain ($|h_s|^2$) is distributed as [20], [21]

$$f_{|h_s|^2}(x) = \frac{m_s^{m_s}}{\Gamma(m_s)} x^{m_s-1} e^{-m_s x}, 0 \leq x < \infty, 0.5 < m < \infty, \tag{2}$$

where the Nakagami parameter $m_s (s \in \{L, N\})$ is an indicator of fading severity where $m_s \to \infty$ indicates no fading while $m_s = 1$ indicates Rayleigh fading. As LOS links would have very few scatterers in millimeter wave frequencies, m_L would tend to be higher while the NLOS parameter m_N would be lower.

Under millimeter wave frequencies, large numbers of antenna elements can be packed within a small area which enables directional beamforming. All different types of nodes are assumed to be capable of performing directional beamforming. Moreover, the antenna patterns of cellular users and D2D transmitters/receivers are assumed to be similar while cellular base stations have a different pattern. To keep the analysis concise, we consider a sectored antenna model [22] where the antenna gain pattern is divided into discrete regions based on the angle off the boresight direction. Thus, the antenna gain ($G_* (* \in \{cb, u\})$ where cb and u respectively denote cellular base stations and all other types of nodes) can be expressed as follows:

$$G_* = \begin{cases} M_* & , |\theta| \leq \frac{\omega_*}{2} \\ m_* & , \text{otherwise} \end{cases}, \tag{3}$$

where ω_* is the antenna beamwidth, θ is the angle off the boresight direction, M_* is the main lobe gain, and m_* is the gain from the side and back lobes. While this gain pattern can be generalized for different side and back lobe gains, and angle dependent main lobe gains, we defer it for future work.

The transmitters and receivers in both cellular and D2D networks perform a beam sweeping process initially in order to estimate the angle of arrival, and we assume that perfect estimation takes place. As such, the combined antenna gains of intended cellular and D2D links are $M_{cb}M_u$ and M_uM_u respectively. The gains of all other links vary randomly depending on the angle off boresight.

C. User Association and Power Control

For the cellular network, each user associates with its closest base station. While other association schemes such as highest received power association may be more favourable, they come at the cost of added complexity and processing power. Moreover, the closest base station is the least likely to suffer from blockages, and thus the most likely to provide the best received signal power. Furthermore, we assume that there only exists at most a single associated user for each base station within a given time-frequency block. Under these assumptions, if the distance between the i-th cellular base station $\phi_{c,b}^i \in \Phi_{c,b}$ and its associated receiver $\phi_{c,u}^i \in \Phi_{c,u}$ is r_c, it has a Rayleigh distribution given by [23]

$$f_{r_c}(x) = 2\pi\lambda_{c,b} x e^{-\pi\lambda_{c,b}x^2}, 0 < x < \infty. \tag{4}$$

In the D2D network, each receiver associates with the corresponding transmitter within its cluster. If this distance is r_{d2d}, its distribution can be expressed as [23]

$$f_{r_{d2d}}(x) = \frac{2x}{R^2}, 0 < x < R. \tag{5}$$

Both cellular and D2D transmitters employ power control which inverts path loss and antenna gains. If P_T is the transmit power, the transmit power to a receiver at distance r can be expressed as $P_T = \frac{\rho c_s r^{\alpha_s}}{M_* M_u}$, where $s \in \{L, N\}$, $* \in \{cb, u\}$, and ρ is the receiver sensitivity. While we assume that that both cellular and D2D receivers have the same sensitivity, different sensitivities can be readily incorporated. Furthermore, we assume that the D2D transmitters are peak power constrained. As such, a D2D transmitter will abort whenever $P_T > P_{d2d}$ where P_{d2d} is the maximum allowable transmit power. The cellular base stations are not assumed to be peak power constrained as they are part of the network infrastructure.

III. Outage Performance

We consider a typical D2D receiver located at a distance of r_{d2d} from its respective transmitter. Without the loss of generality, we consider that this receiver is located at the origin. The outage probability (P_O) is defined as $P_O = \Pr[\gamma < \gamma_{th}]$, where γ is the signal to interference and noise ratio (SINR) at the D2D receiver while γ_{th} is the SINR reception threshold of the receiver. The SINR can be written as

$$\gamma = \frac{P_s |h_s|^2 M_u^2 c_s^{-1} r_{d2d}^{-\alpha_s}}{I_c + I_{d2d} + N}, \tag{6}$$

where P_s is the transmit power, I_c is the interference from cellular base stations, I_{d2d} is the interference from other D2D transmitters, and N is the noise power. It is clearly seen that γ varies with the LOS and NLOS nature of the link. Therefore, we can separate the LOS and NLOS cases and express P_O as

$$\begin{aligned} P_O &= \mathbb{E}[a_l P_{O,L} + a_N P_{O,N}] \\ &= \frac{2P_{O,L}}{\beta^2 R^2}\left(1 - e^{-\beta R}(\beta R + 1)\right) \\ &\quad + P_{O,N}\left(1 - \frac{2}{\beta^2 R^2}\left(1 - e^{-\beta R}(\beta R + 1)\right)\right), \end{aligned} \tag{7}$$

where $a_l = e^{-\beta r_{d2d}}$ is the probability of the link being LOS, $a_N = 1 - e^{-\beta r_{d2d}}$ is the probability of the link being NLOS, while $P_{O,L}$ and $P_{O,N}$ are respectively the outages given LOS and NLOS links.

1) Deriving $P_{O,L}$: When a LOS link exists between the D2D transmitter and receiver given a certain r_{d2d}, we can express $P_{O,L}$ as

$$P_{O,L} = \Pr\left[\frac{P_L |h_L|^2 M_u^2 c_L^{-1} r_{d2d}^{-\alpha_L}}{I_c + I_{d2d} + N} < \gamma_{th}\right]. \tag{8}$$

The transmit power P_L is given by

$$P_L = \begin{cases} \frac{\rho c_L r_{d2d}^{\alpha_L}}{M_u^2} & , \frac{\rho c_L r_{d2d}^{\alpha_L}}{M_u^2} < P_{d2d} \\ 0 & , \text{otherwise} \end{cases}. \tag{9}$$

Let τ_L be the probability that $P_L = \frac{\rho c_L r_{d2d}^{\alpha_L}}{M_u^2}$. Thus, we can express $\tau_L = \Pr\left[r_{d2d} < \left(\frac{P_{d2d}M_u^2}{\rho c_L}\right)^{\frac{1}{\alpha_L}}\right]$ as

$$\tau_L = \begin{cases} \frac{1}{R^2}\left(\frac{P_{d2d}M_u^2}{\rho c_L}\right)^{\frac{2}{\alpha_L}} & , \text{if } \left(\frac{P_{d2d}M_u^2}{\rho c_L}\right)^{\frac{1}{\alpha_L}} < R \\ 1 & , \text{if } \left(\frac{P_{d2d}M_u^2}{\rho c_L}\right)^{\frac{1}{\alpha_L}} > R \end{cases}. \quad (10)$$

Now, getting back to the objective of deriving $P_{O,L}$, we can express (8) for integer m_l as

$$P_{O,L} = 1 - \tau_L + \tau_L \Pr\left[|h_L|^2 < \frac{\gamma_{th}(I_c + I_{d2d} + N)}{\rho}\right]$$
$$= 1 - \tau_L \mathbb{E}\left[\frac{\Gamma\left(m_L, m_L\frac{\gamma_{th}(I_c+I_{d2d}+N)}{\rho}\right)}{\Gamma(m_L)}\right]$$
$$= 1 - \tau_L \mathbb{E}_I\left[\frac{1}{\Gamma(m_L)}\int_{\frac{m_L\gamma_{th}(I_c+I_{d2d}+N)}{\rho}}^{\infty} y^{m_L-1}e^{-y}dy\right]$$
$$= 1 - \tau_L \mathbb{E}_I\left[e^{-\frac{m_L\gamma_{th}(I_c+I_{d2d}+N)}{\rho}}\sum_{\nu=0}^{m_L-1}\frac{1}{\nu!}\left(\frac{m_L\gamma_{th}(I_c+I_{d2d}+N)}{\rho}\right)^{\nu}\right]$$
$$= 1 - \tau_L e^{-\frac{m_L\gamma_{th}N}{\rho}}\sum_{\nu=0}^{m_L-1}\frac{1}{\nu!}\left(\frac{m_L\gamma_{th}}{\rho}\right)^{\nu}\sum_{\mu=0}^{\nu}\binom{\nu}{\mu}N^{\nu-\mu}$$
$$\times \sum_{\kappa=0}^{\mu}\binom{\mu}{\kappa}\mathbb{E}_{I_c}\left[I_c^{\kappa}e^{-\frac{m_L\gamma_{th}I_c}{\rho}}\right]\mathbb{E}_{I_{d2d}}\left[I_{d2d}^{\mu-\kappa}e^{-\frac{m_L\gamma_{th}I_{d2d}}{\rho}}\right]$$
$$= 1 - \tau_L e^{-\frac{m_L\gamma_{th}N}{\rho}}\sum_{\nu=0}^{m_L-1}\frac{1}{\nu!}\left(\frac{m_L\gamma_{th}}{\rho}\right)^{\nu}\sum_{\mu=0}^{\nu}\binom{\nu}{\mu}N^{\nu-\mu}\sum_{\kappa=0}^{\mu}\binom{\mu}{\kappa}$$
$$\times (-1)^{\kappa}M_{I_c}^{(\kappa)}\left(s|_{s=\frac{m_L\gamma_{th}}{\rho}}\right)(-1)^{\mu-\kappa}M_{I_{d2d}}^{(\mu-\kappa)}\left(s|_{s=\frac{m_L\gamma_{th}}{\rho}}\right) \quad (11)$$

2) Deriving $P_{O,N}$: In a similar way to $P_{O,L}$, $P_{O,N}$ can be derived as

$$P_{O,N} = 1 - \tau_N e^{-\frac{m_N\gamma_{th}N}{\rho}}\sum_{\nu=0}^{m_N-1}\frac{1}{\nu!}\left(\frac{m_N\gamma_{th}}{\rho}\right)^{\nu}$$
$$\times \sum_{\mu=0}^{\nu}\binom{\nu}{\mu}N^{\nu-\mu}\sum_{\kappa=0}^{\mu}\binom{\mu}{\kappa}(-1)^{\kappa}M_{I_c}^{(\kappa)}\left(s|_{s=\frac{m_N\gamma_{th}}{\rho}}\right)$$
$$\times (-1)^{\mu-\kappa}M_{I_{d2d}}^{(\mu-\kappa)}\left(s|_{s=\frac{m_N\gamma_{th}}{\rho}}\right), \quad (12)$$

where τ_N is given by

$$\tau_N = \begin{cases} \frac{1}{R^2}\left(\frac{P_{d2d}M_u^2}{\rho c_N}\right)^{\frac{2}{\alpha_N}} & , \text{if } \left(\frac{P_{d2d}M_u^2}{\rho c_N}\right)^{\frac{1}{\alpha_N}} < R \\ 1 & , \text{if } \left(\frac{P_{d2d}M_u^2}{\rho c_N}\right)^{\frac{1}{\alpha_N}} > R \end{cases}. \quad (13)$$

IV. Interference Characteristics

In this section, we derive the MGFs of the interference from both cellular and other D2D transmitters M_{I_c} and $M_{I_{d2d}}$. For both cellular and D2D networks, we assume that all transmitters/base stations are actively engaged in transmission. This assumption is valid since they have a significantly lower spatial density compared to the relevant receivers. Moreover, independent thinning can be easily used to remove non-active base stations/transmitters.

A. Interference from Cellular Transmitters

The interference from transmitting cellular base stations I_c can be divided into two separate terms composed of LOS and NLOS cellular base stations using the thinning property [24]. If $I_{c,L}$ and $I_{c,N}$ denote these two terms, $I_c = I_{c,L} + I_{c,N}$. Moreover, $M_{I_c} = M_{I_{c,L}}M_{I_{c,N}}$ due to the independence of thinned Poisson point processes [24].

1) Deriving $M_{I_{c,L}}$: In order to derive $M_{I_{c,L}}$ we first transform the process of interfering LOS base stations to an equivalent inhomogeneous Poisson point process which incorporates the path loss exponent, antenna gains, transmit power, and fading. Let r be the distance from the i-th cellular base station $\phi_{c,b}^i$ to the considered D2D receiver. While the field of cellular base stations $\Phi_{c,b}$ exists in $\mathbb{R}^2$ as a homogeneous Poisson point process, it can be mapped to an equivalent 1-D inhomogeneous Poisson point process [24] with density $\tilde{\lambda}_{c,b}$ where

$$\tilde{\lambda}_{c,b} = 2\pi\lambda_{c,b}r, 0 < r < \infty. \quad (16)$$

The cellular base station $\phi_{c,b}^i$ is LOS from the D2D receiver with a probability of $e^{-\beta r}$. While this probability depends on r, it is independent from the positions of other cellular base stations. As such, the Colouring Theorem [24] can be used to perform independent thinning of $\Phi_{c,b}$ to obtain the process of LOS cellular base stations as an inhomogeneous Poisson point process with density $\tilde{\lambda}_{c,bL} = e^{-\beta r}\tilde{\lambda}_{c,b} = 2\pi\lambda_{c,b}e^{-\beta r}r$.

Using the Mapping Theorem further [24], this thinned 1-D Poisson process can be mapped to an equivalent 1-D Poisson process in terms of interference statistics where the path loss exponent is 1 [25]. The density of the resultant process $\hat{\lambda}_{c,bL}$ is given by

$$\hat{\lambda}_{c,bL} = \frac{2\pi\lambda_{c,b}e^{-\beta r^{\frac{1}{\alpha_L}}}r^{\frac{2}{\alpha_L}-1}}{\alpha_L}, 0 < r < \infty. \quad (17)$$

Next, we go one step further and incorporate the transmit power of $\phi_{c,b}^i$, the antenna gains of $\phi_{c,b}^i$ and the D2D receiver, and the fading between $\phi_{c,b}^i$ and the D2D receiver to the process of LOS cellular base stations [25]. Thus, the resultant process has a density $\bar{\lambda}_{c,bL}$ which can be expressed as

$$\bar{\lambda}_{c,bL} = \mathbb{E}_{P_{cL}G_{cb}G_u|h_{cL}|^2}\left[P_{cL}|h_{cL}|^2\hat{\lambda}_{c,bL}(P_{cL}G_{cb}G_u|h_{cL}|^2 r)\right]$$
$$= \frac{2\pi\lambda_{c,b}r^{\frac{2}{\alpha_L}-1}}{\alpha_L}\sum_{k=0}^{\infty}\frac{(-\beta r^{\frac{1}{\alpha_L}})^k}{k!}$$
$$\times \mathbb{E}\left[P_{cL}^{\frac{2+k}{\alpha_L}}\right]\mathbb{E}\left[G_{cb}^{\frac{2+k}{\alpha_L}}\right]\mathbb{E}\left[G_u^{\frac{2+k}{\alpha_L}}\right]\mathbb{E}\left[(|h_{cL}|^2)^{\frac{2+k}{\alpha_L}}\right], \quad (18)$$

where P_{cL} is the transmit power of the base station $\phi_{c,b}^i$, G_{cb} is the gain of $\phi_{c,b}^i$, G_u is the gain of the D2D receiver, and $|h_{cL}|^2$ is the small scale fading channel gain between $\phi_{c,b}^i$ and the D2D receiver.

In order to evaluate (18), the distribution of P_{cL} is required, which in turn depends on whether the associated cellular user to $\phi_{c,b}^i$ is within LOS or not. The associated receiver $\phi_{c,u}^i$ is LOS to $\phi_{c,b}^i$ with probability $e^{-\beta r_c}$, and NLOS with probability $1 - e^{-\beta r_c}$, where r_c is the distance between $\phi_{c,u}^i$

$$\mathbb{U}_{c,L} = \frac{\rho^{\frac{2+k}{\alpha_L}}\Gamma\left(m_L+\frac{2+k}{\alpha_L}\right)}{4\pi^2\Gamma(m_L)m_L^{-\frac{2+k}{\alpha_L}}(M_u M_{cb})^{\frac{2+k}{\alpha_L}}}\left(\theta_{cb}M_{cb}^{\frac{2+k}{\alpha_L}}+(2\pi-\theta_{cb})m_{cb}^{\frac{2+k}{\alpha_L}}\right)\left(\theta_u M_u^{\frac{2+k}{\alpha_L}}+(2\pi-\theta_u)m_u^{\frac{2+k}{\alpha_L}}\right)\left(\frac{c_L^{\frac{2+k}{\alpha_L}}}{(\pi\lambda_{c,b})^{\frac{3+k}{2}}}\left(\sqrt{\pi\lambda_{c,b}}\Gamma\left(\frac{k+2}{2}\right){}_1\mathcal{F}_1\left(\frac{k+2}{2};\frac{1}{2};\frac{\beta^2}{4\pi\lambda_{c,b}}\right)-\beta\Gamma\left(\frac{k+5}{2}\right)\right.\right.$$
$$\left.\left.\times\ {}_1\mathcal{F}_1\left(\frac{k+5}{2};\frac{3}{2};\frac{\beta^2}{4\pi\lambda_{c,b}}\right)\right)+\frac{c_N^{\frac{2+k}{\alpha_L}}}{(\pi\lambda_{c,b})^{\frac{\alpha_L+\alpha_N(2+k)}{2\alpha_L}}}\left(-\sqrt{\pi\lambda_{c,b}}\Gamma\left(1+\frac{(2+k)\alpha_N}{2\alpha_L}\right)\left({}_1\mathcal{F}_1\left(1+\frac{(2+k)\alpha_N}{2\alpha_L};\frac{1}{2};\frac{\beta^2}{4\pi\lambda_{c,b}}\right)-1\right)+\beta\Gamma\left(\frac{3}{2}+\frac{(2+k)\alpha_N}{2\alpha_L}\right){}_1\mathcal{F}_1\left(\frac{3}{2}+\frac{(2+k)\alpha_N}{2\alpha_L};\frac{3}{2};\frac{\beta^2}{4\pi\lambda_{c,b}}\right)\right)\right) \quad (14)$$

$$\mathbb{U}_{c,N} = \frac{\rho^{\frac{2+k}{\alpha_N}}\Gamma\left(m_N+\frac{2+k}{\alpha_N}\right)}{4\pi^2\Gamma(m_N)m_N^{-\frac{2+k}{\alpha_N}}(M_u M_{cb})^{\frac{2+k}{\alpha_N}}}\left(\frac{c_L^{\frac{2+k}{\alpha_N}}}{(\pi\lambda_{c,b})^{\frac{\alpha_N+\alpha_L(2+k)}{\alpha_N}}}\left(\sqrt{\pi\lambda_{c,b}}\Gamma\left(\frac{(k+2)\alpha_L}{2\alpha_N}\right){}_1\mathcal{F}_1\left(\frac{(k+2)\alpha_L}{2\alpha_N};\frac{1}{2};\frac{\beta^2}{4\pi\lambda_{c,b}}\right)-\beta\Gamma\left(\frac{3}{2}+\frac{(2+k)\alpha_L}{2\alpha_N}\right){}_1\mathcal{F}_1\left(\frac{3}{2}+\frac{(2+k)\alpha_L}{2\alpha_N};\frac{3}{2};\frac{\beta^2}{4\pi\lambda_{c,b}}\right)\right)\right.$$
$$\left.+\frac{c_N^{\frac{2+k}{\alpha_N}}}{(\pi\lambda_{c,b})^{\frac{3+k}{2}}}\left(-\sqrt{\pi\lambda_{c,b}}\Gamma\left(1+\frac{2+k}{2}\right)\left({}_1\mathcal{F}_1\left(1+\frac{2+k}{2};\frac{1}{2};\frac{\beta^2}{4\pi\lambda_{c,b}}\right)-1\right)+\beta\Gamma\left(\frac{k+5}{2}\right){}_1\mathcal{F}_1\left(\frac{k+5}{2};\frac{3}{2};\frac{\beta^2}{4\pi\lambda_{c,b}}\right)\right)\right)\left(\theta_{cb}M_{cb}^{\frac{2+k}{\alpha_N}}+(2\pi-\theta_{cb})m_{cb}^{\frac{2+k}{\alpha_N}}\right)\left(\theta_u M_u^{\frac{2+k}{\alpha_N}}+(2\pi-\theta_u)m_u^{\frac{2+k}{\alpha_N}}\right) \quad (15)$$

and $\phi_{c,b}^i$. These probabilities are independent from whether $\phi_{c,b}^i$ and the D2D receiver are LOS or not. Thus, P_{cL} can be expressed as follows:

$$P_{cL} = \begin{cases} \frac{\rho c_L r_c^{\alpha_L}}{M_U M_{cb}^{\alpha_N}} & , \phi_{c,u}^i \text{ and } \phi_{c,b}^i \text{ are LOS} \\ \frac{\rho c_N r_c^{\alpha_N}}{M_U M_{cb}} & , \phi_{c,u}^i \text{ and } \phi_{c,b}^i \text{ are NLOS} \end{cases}. \quad (19)$$

After substituting $\mathbb{E}_{|h_{cL}|^2}\left[\left(|h_{cL}|^2\right)^{\frac{2+k}{\alpha_L}}\right]$ and $\mathbb{E}_{P_{cL}}\left[P_{cL}^{\frac{2+k}{\alpha_L}}\right]$ to (18), we obtain the final expression for $\bar{\lambda}_{c,bL}$ as

$$\bar{\lambda}_{c,bL} = \sum_{k=0}^{\infty}\frac{2\pi\lambda_{c,b}(-\beta)^k r^{\frac{2+k}{\alpha_L}-1}}{\alpha_L k!}\mathbb{U}_{c,L}, 0<r<\infty, \quad (20)$$

where $\mathbb{U}_{c,L}$ is given in (14).

We now return to our origin objective of deriving $M_{I_{c,L}} = \mathbb{E}[e^{-sI_{c,L}}]$. Due to the mapping, the interference power from a single cellular base station $\phi_{c,b}^i$ within the resultant process reduces to $(c_L r)^{-1}$. Note that the path loss exponent has reduced to 1 while the gains, fading, and transmit powers are absent. Thus, using the Campbell's Theorem [24], $M_{I_{c,L}}$ is expressed as

$$M_{I_{c,L}} = e^{\left(\int_0^\infty\left(e^{-s(c_L r)^{-1}}-1\right)\bar{\lambda}_{c,bL}dr\right)} = e^{\sum_{k=0}^{\infty}\frac{2\pi\lambda_{c,b}(-\beta)^k}{\alpha_L k!}\left(\frac{s}{c_L}\right)^{\frac{2+k}{\alpha_L}}\Gamma\left(-\frac{2+k}{\alpha_L}\right)\mathbb{U}_{c,L}}. \quad (21)$$

2) Deriving $M_{I_{c,N}}$: Using similar arguments as with the derivation of $M_{I_{c,L}}$, $M_{I_{c,N}}$ ca be written as

$$M_{I_{c,N}} = e^{\sum_{k=1}^{\infty}-\frac{2\pi\lambda_{c,b}(-\beta)^k}{\alpha_N k!}\left(\frac{s}{c_N}\right)^{\frac{2+k}{\alpha_N}}\Gamma\left(-\frac{2+k}{\alpha_N}\right)\mathbb{U}_{c,N}}, \quad (22)$$

where $\mathbb{U}_{c,N}$ is given in (15).

B. Interference from other D2D transmitters

The interference from other D2D transmitters on the D2D receiver in question can be decomposed into LOS ($I_{d2d,L}$) and NLOS ($I_{d2d,N}$) components with $I_{d2d} = I_{d2d,L} + I_{d2d,N}$ and $M_{I_{d2d}} = M_{I_{d2d,L}} M_{I_{d2d,N}}$.

1) Deriving $M_{I_{d2d,L}}$: While the derivation of $M_{I_{d2d,L}}$ is similar to $M_{I_{c,L}}$ and $M_{I_{c,N}}$, a complication arises while obtaining the $\frac{2+k}{\alpha}$-th moment of the transmit power of a D2D transmitter (P_{dL}). If r_d is the distance from a D2D transmitter to the associated receiver, P_{dL} takes $\frac{\rho c_L r_d^{\alpha_L}}{M_u^2}$ with probability $e^{-\beta r_d}\tau_L$, $\frac{\rho c_N r_d^{\alpha_N}}{M_u^2}$ with probability $(1-e^{-\beta r_d})\tau_N$, and 0 with probability $e^{-\beta r_d}(1-\tau_L)+(1-e^{-\beta r_d})(1-\tau_N)$ after considering blockages and peak power constraints. Moreover, while τ_L (10) and τ_N (13) can take multiple combinations as evident from their expressions, we consider the case where $\max\left(\left(\frac{P_{d2d}M_u^2}{\rho c_N}\right)^{\frac{1}{\alpha_N}},\left(\frac{P_{d2d}M_u^2}{\rho c_L}\right)^{\frac{1}{\alpha_L}}\right) < R$ for this paper.

After using the Slivnyak's theorem [24] to remove the desired transmitter from the field of interferers, $M_{I_{d2d,L}}$ is expressed as

$$M_{I_{d2d,L}} = e^{\sum_{k=0}^{\infty}\frac{2\pi\lambda_{d,t}(-\beta)^k}{\alpha_L k!}\left(\frac{s}{c_L}\right)^{\frac{2+k}{\alpha_L}}\Gamma\left(-\frac{2+k}{\alpha_L}\right)\mathbb{U}_{d,L}}, \quad (23)$$

where $\mathbb{U}_{d,L}$ is given in (25).

2) Deriving $M_{I_{d2d,N}}$: The expression for $M_{I_{d2d,N}}$ is obtained as

$$M_{I_{d2d,N}} = e^{\sum_{k=1}^{\infty}-\frac{2\pi\lambda_{d,t}(-\beta)^k}{\alpha_N k!}\left(\frac{s}{c_N}\right)^{\frac{2+k}{\alpha_N}}\Gamma\left(-\frac{2+k}{\alpha_N}\right)\mathbb{U}_{d,N}}. \quad (24)$$

V. Numerical Results

We next present performance trends of millimeter wave D2D networks for several system parameter configurations. The details of the simulation setup are as follows. A 100MHz bandwidth is considered (with a resultant noise power of -94 dBm) in the 28 GHz band along with intercepts $cL = cN = 10^5$, and path loss exponents $\alpha_L = 2.1$ and $\alpha_N = 4.1$. Moreover, $\lambda_{c,b} = 10^{-4}$, $\theta_c = \theta_u = \frac{\pi}{10}$, $M_c = 20$ dB, $m_c = m_u = -10$ dB, $\rho = -80$ dBm, and $\beta = 0.001$.

Fig. 1 plots the outage probability with respect to the SINR threshold γ_{th}. It is clearly seen that D2D operation is infeasible when $\gamma_{th} > 20$ dB. For millimeter wave D2D networks, four major factors affect the overall outage of a D2D receiver: interference from cellular base stations, interference from other D2D transmitters, thermal noise due to the high bandwidth, and the outage due to the associated transmitter being cut-off due to the peak power constraint. When $M_u = 10$ dB, increasing the cluster radius R generally increases the outage

$$\mathbb{U}_{d,L} = \frac{1}{2\pi^2 R^2}\left(\frac{\rho}{M_u^2}\right)^{\frac{2+k}{\alpha_L}} \frac{\Gamma\left(m_L + \frac{2+k}{\alpha_L}\right)}{\Gamma(m_L) m_L^{-\frac{2+k}{\alpha_L}}} \left(\frac{c_L^{\frac{2+k}{\alpha_L}}}{\beta^{4+k}} \left(\Gamma(4+k) - \Gamma\left(4+k, \beta\left(\frac{P_{d2d} M_u^2}{c_L \rho}\right)^{\frac{1}{\alpha_L}}\right)\right) + \frac{c_N^{\frac{2+k}{\alpha_L}}}{(2\alpha_L + (2+k)\alpha_N)\beta^{\frac{2\alpha_L+(2+k)\alpha_N}{\alpha_L}}} \left(\alpha_L \left(\beta \left(\frac{P_{d2d} M_u^2}{c_N \rho}\right)^{\frac{1}{\alpha_N}}\right)^{\frac{2\alpha_L+(2+k)\alpha_N}{\alpha_L}} \right.\right.$$
$$\left.\left. -(2\alpha_L + (2+k)\alpha_N) \left(\Gamma\left(\frac{2\alpha_L + (2+k)\alpha_N}{\alpha_L}\right) - \Gamma\left(\frac{2\alpha_L + (2+k)\alpha_N}{\alpha_L}, \beta\left(\frac{P_{d2d} M_u^2}{c_N \rho}\right)^{\frac{1}{\alpha_N}}\right)\right)\right)\right) \left(\theta_u M_u^{\frac{2+k}{\alpha_L}} + (2\pi - \theta_u) m_u^{\frac{2+k}{\alpha_L}}\right)^2 \tag{25}$$

$$\mathbb{U}_{d,N} = \frac{1}{2\pi^2 R^2}\left(\frac{\rho}{M_u^2}\right)^{\frac{2+k}{\alpha_N}} \frac{\Gamma\left(m_N + \frac{2+k}{\alpha_N}\right)}{\Gamma(m_N) m_N^{-\frac{2+k}{\alpha_N}}} \left(\frac{c_L^{\frac{2+k}{\alpha_N}}}{\beta^{\frac{2\alpha_N+(2+k)\alpha_L}{\alpha_N}}} \left(\Gamma\left(\frac{2\alpha_N + (2+k)\alpha_L}{\alpha_N}\right) - \Gamma\left(\frac{2\alpha_N + (2+k)\alpha_L}{\alpha_N}, \beta\left(\frac{P_{d2d} M_u^2}{c_L \rho}\right)^{\frac{1}{\alpha_L}}\right)\right) + \frac{c_N^{\frac{2+k}{\alpha_N}}}{(4+k)\beta^{4+k}} \left(\left(\beta \left(\frac{P_{d2d} M_u^2}{c_N \rho}\right)^{\frac{1}{\alpha_N}}\right)^{4+k} \right.\right.$$
$$\left.\left. -(4+k) \left(\Gamma(4+k) - \Gamma\left(4+k, \beta\left(\frac{P_{d2d} M_u^2}{c_N \rho}\right)^{\frac{1}{\alpha_N}}\right)\right)\right)\right) \left(\theta_u M_u^{\frac{2+k}{\alpha_N}} + (2\pi - \theta_u) m_u^{\frac{2+k}{\alpha_N}}\right)^2 \tag{26}$$

probability. This is due to two reasons. First, a higher radius causes other D2D transmitters to transmit at a higher power level, increasing interference. This effect is amplified due to the fact that the probability of a NLOS link increases with the cell radius. Second, as the cell radius increases, the desired link itself has an increased tendency to be NLOS, resulting in more severe fading and being cut-off due to the required power exceeding the peak power threshold. However, when M_u is increased to 20 dB, the trend is unclear. As R is increased, the outage roughly drops and then increases again. This is due to two competing effects occurring for a M_u value; the desired link would have a lower probability to get cut-off due to the lower transmit power needed, and the intra-D2D interference increases because a lesser number of interfering D2D transmitters get cut-off. At a certain radius, the effect of the latter outweighs the former, and the outage increases. Moreover, it is important to note that the R and M_u pair providing the best performance also depends on the specific SINR threshold γ_{th}.

The outage probability is plotted against the D2D transmitter density $\lambda_{d,t}$ in Fig. 2. While a higher $\lambda_{d,t}$ causes the outage to approach 1 due to intra-D2D interference, reducing $\lambda_{d,t}$ causes the outage to first drop abruptly, and then flatten out towards a value determined by noise and inter-network interference. Interestingly, note that the outage probability increases when m_L is increased from 2 to 4. While this may seem counter-intuitive, this phenomenon occurs due to the intra-D2D interference being less severely faded. However, the change in the outage when m_N changes is negligible, and the curves for $m_N = 1$ and $m_N = 2$ almost overlap. Moreover, it's interesting to note that while a lower P_{d2d} provides a lower outage at very low $\lambda_{d,t}$ values, the converse is true when $\lambda_{d,t}$ increases. As P_{d2d} is lower, more D2D transmitters requiring additional power to transmit due to the increased radius get cut-off; thus reducing interference. However, under this scenario, the desired link also has an increased cut-off probability, which becomes more prominent when $\lambda_{d,t}$ is high. This is because for high $\lambda_{d,t}$, its contribution to the interference outweighs the interference reduction caused by a lower P_{d2d}.

We investigate the effect of the peak D2D transmit power P_{d2d} on the outage in Fig. 3. While P_{d2d} increases, the outage first drops, and then approaches 1. As such, there is an optimum P_{d2d} which gives the best performance. Furthermore, it is observed that a change in the receiver sensitivity ρ does not significantly change the performance characteristics except shifting the location of the minimum outage; a higher ρ provides the best performance at a higher P_{d2d} and vice-versa.

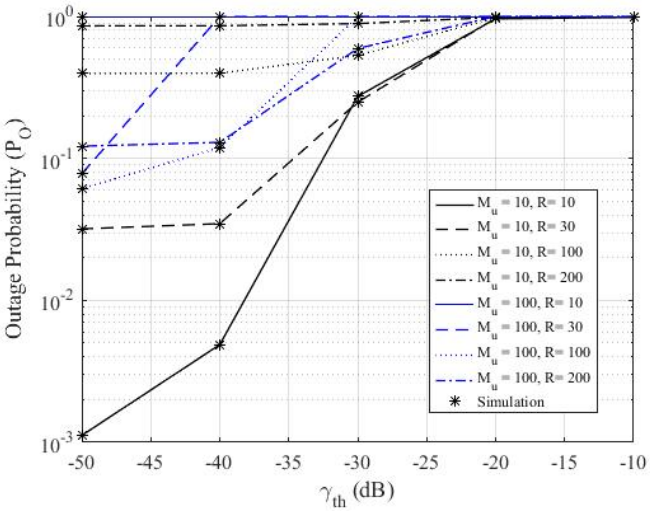

Fig. 1: The outage probability (P_O) vs. γ_{th} in dB for different D2D cell radii (R) and M_u. $\lambda_{d,t} = 10^{-4}$, $m_L = 4$, $m_N = 2$, and $P_{d2d} = -10$ dBm.

VI. Conclusion

The performance of a random D2D network underlaying a millimeter wave cellular network was characterized within this paper. Homogeneous Poisson processes were considered for the cellular base stations and users while a Matern cluster process was considered for the D2D network nodes. Sectored antenna patterns and random blockages were considered alongside different path loss exponents and Nakagami fading indexes depending on the LOS or NLOS nature of a link. The cellular users were assumed to connect with their closest base station while D2D receivers within a cluster connect with the transmitter represented by the cluster head. Moreover, path loss and antenna gain inversion based power control, varying upon the LOS or NLOS nature is employed by both networks while D2D transmitters are also peak power constrained. The MGFs of interference to a D2D receiver device from the cellular base stations and other D2D transmitters are derived in

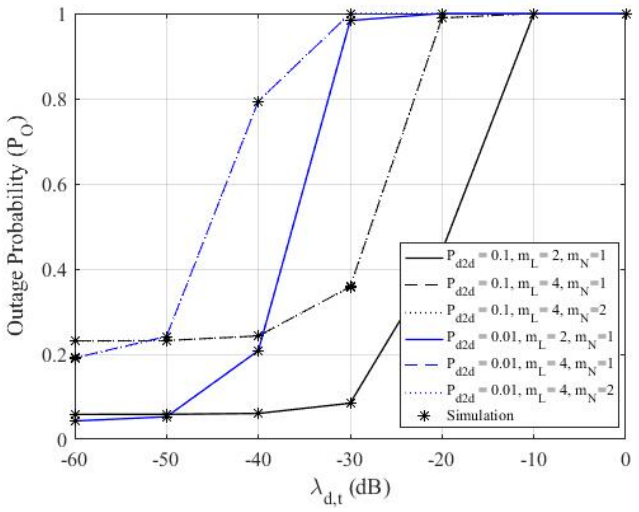

Fig. 2: The outage probability (P_O) vs. the D2D transmitter density $\lambda_{d,t}$ in dB under varying m_L, m_N, and P_{d2d}. $\gamma_{th} = 10^{-3}$, $R = 20$, and $M_u = 10\,\text{dB}$.

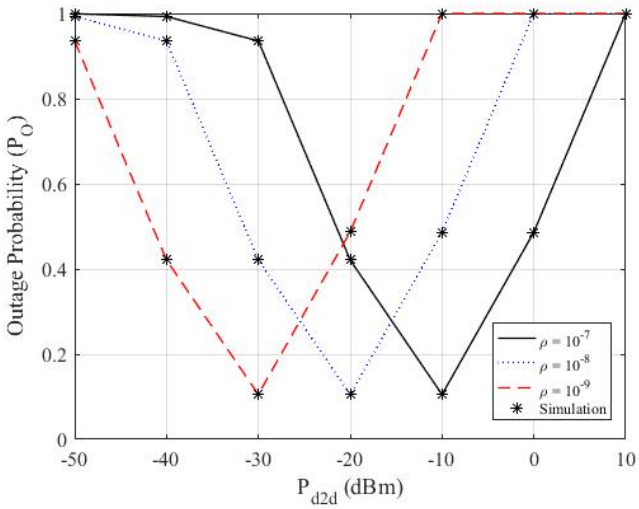

Fig. 3: The outage probability (P_O) vs. the peak D2D power level P_{d2d} under different receiver thresholds ρ. $\gamma_{th} = 10^{-3}$, $R = 100$, and $M_u = 20\,\text{dB}$, $m_L = 2$, $m_N = 1$, and $\lambda_{d,t} = 10^{-4}$.

closed-form, and are used to obtain the outage probability of a D2D receiver. It is observed that the outage has a complex relationship with the D2D cluster radius and antenna gains. Furthermore, a minima of the outage is occurs for a specific D2D peak power threshold, while a higher LOS fading severity (lower m_L) also reduces the outage. Extensions of the work include considering alternate transmitter-receiver association schemes and power control schemes.

REFERENCES

[1] D. Liu, L. Wang, Y. Chen, M. Elkashlan, K. K. Wong, R. Schober, and L. Hanzo, "User association in 5g networks: A survey and an outlook," *IEEE Commun. Surveys and Tut.*, vol. 18, no. 2, pp. 1018–1044, Secondquarter 2016.

[2] T. S. Rappaport, S. Sun, R. Mayzus, H. Zhao, Y. Azar, K. Wang, G. N. Wong, J. K. Schulz, M. Samimi, and F. Gutierrez, "Millimeter wave mobile communications for 5g cellular: It will work!" *IEEE Access*, vol. 1, pp. 335–349, 2013.

[3] T. Bai and R. W. Heath, "Coverage and rate analysis for millimeter-wave cellular networks," *IEEE Trans. Wireless Commun.*, vol. 14, no. 2, pp. 1100–1114, Feb 2015.

[4] C.-X. Wang, F. Haider, X. Gao, X.-H. You, Y. Yang, D. Yuan, H. Aggoune, H. Haas, S. Fletcher, and E. Hepsaydir, "Cellular architecture and key technologies for 5G wireless communication networks," *IEEE Commun. Magazine*, vol. 52, no. 2, pp. 122–130, February 2014.

[5] J. Qiao, X. S. Shen, J. W. Mark, Q. Shen, Y. He, and L. Lei, "Enabling device-to-device communications in millimeter-wave 5G cellular networks," *IEEE Commun. Mag.*, vol. 53, no. 1, pp. 209–215, January 2015.

[6] A. Gupta and R. K. Jha, "A survey of 5G network: Architecture and emerging technologies," *IEEE Access*, vol. 3, pp. 1206–1232, 2015.

[7] D. Maamari, N. Devroye, and D. Tuninetti, "Coverage in mmwave cellular networks with base station co-operation," *IEEE Trans. Wireless Commun.*, vol. 15, no. 4, pp. 2981–2994, April 2016.

[8] W. Lu and M. D. Renzo, "Accurate stochastic geometry modeling and analysis of mmwave cellular networks," in *Proc. IEEE ICUWB*, Oct 2015, pp. 1–5.

[9] K. Venugopal, M. C. Valenti, and R. W. Heath, "Device-to-device millimeter wave communications: Interference, coverage, rate, and finite topologies," *IEEE Trans. on Wireless Commun.*, vol. 15, no. 9, pp. 6175–6188, Sept 2016.

[10] Y. Niu, L. Su, C. Gao, Y. Li, D. Jin, and Z. Han, "Exploiting device-to-device communications to enhance spatial reuse for popular content downloading in directional mmwave small cells," *IEEE Trans. Veh. Technol.*, vol. 65, no. 7, pp. 5538–5550, July 2016.

[11] M. Mirahsan, R. Schoenen, S. S. Szyszkowicz, and H. Yanikomeroglu, "Measuring the spatial heterogeneity of outdoor users in wireless cellular networks based on open urban maps," in *Proc. IEEE ICC*, June 2015, pp. 2834–2838.

[12] Z. Guizani and N. Hamdi, "mmwave E-band D2D communications for 5G-underlay networks: Effect of power allocation on d2d and cellular users throughputs," in *Proc. IEEE ISCC*, June 2016, pp. 114–118.

[13] I. Gradshteyn and I. Ryzhik, *Table of integrals, Series, and Products*, 7th ed. Academic Press, 2007.

[14] Z. Chen, C.-X. Wang, X. Hong, J. Thompson, S. Vorobyov, X. Ge, H. Xiao, and F. Zhao, "Aggregate interference modeling in cognitive radio networks with power and contention control," *IEEE Trans. Commun.*, vol. 60, no. 2, pp. 456–468, Feb. 2012.

[15] E. Salbaroli and A. Zanella, "Interference analysis in a Poisson field of nodes of finite area," *IEEE Trans. Veh. Technol.*, vol. 58, no. 4, pp. 1776–1783, May 2009.

[16] A. Baddeley, I. Barany, R. Schneider, and W. Weil, *Spatial Point Processes and their Applications*. Springer, 2007.

[17] Y. Liu, C. Yin, J. Gao, and X. Sun, "Transmission capacity for overlaid wireless networks: A homogeneous primary network versus an inhomogeneous secondary network," in *Proc. IEEE ICCCAS*, vol. 1, Nov 2013, pp. 154–158.

[18] T. Bai, R. Vaze, and R. W. Heath, "Analysis of blockage effects on urban cellular networks," *IEEE Trans. Wireless Commun.*, vol. 13, no. 9, pp. 5070–5083, Sept 2014.

[19] G. R. MacCartney, J. Zhang, S. Nie, and T. S. Rappaport, "Path loss models for 5G millimeter wave propagation channels in urban microcells," in *Proc. IEEE GLOBECOM*, Dec 2013, pp. 3948–3953.

[20] C. Tellambura, A. Annamalai, and V. K. Bhargava, "Closed form and infinite series solutions for the MGF of a dual-diversity selection combiner output in bivariate Nakagami fading," *IEEE Transactions on Communications*, vol. 51, no. 4, pp. 539–542, April 2003.

[21] A. Molisch, *Wireless Communications*. Wiley-IEEE Press, 2011.

[22] M. D. Renzo, "Stochastic geometry modeling and analysis of multi-tier millimeter wave cellular networks," *IEEE Trans. Wireless Commun.*, vol. 14, no. 9, pp. 5038–5057, Sept 2015.

[23] S. Kusaladharma and C. Tellambura, "Massive MIMO based underlay networks with power control," in *Proc. IEEE ICC*, May 2016, pp. 1–6.

[24] J. F. Kingman, *Poisson Processes*. Oxford University Press, 1993.

[25] S. Kusaladharma, P. Herath, and C. Tellambura, "Underlay interference analysis of power control and receiver association schemes," *IEEE Trans. Veh. Technol.*, vol. PP, no. 99, pp. 1–1, 2016.